ACS SENSORS

pubs.acs.org/acssensors Article

Simple Tripedal DNA Walker Prepared by Target-Triggered Catalytic Hairpin Assembly for Ultrasensitive Electrochemiluminescence Detection of MicroRNA

Li Wang,* Pengfei Liu, Zhijun Liu, Kairen Zhao, Shuying Ye, Guoxi Liang, and Jun-Jie Zhu*

Cite This: https://dx.doi.org/10.1021/acssensors.0c01864 Read Online

ACCESS | Metrics & More | Article Recommendations | Supporting Information

ABSTRACT: In contrast to common DNA walkers, multipedal DNA walkers exhibit larger walking area and faster walking kinetics and provide increased amplification efficiency. Consequently, they have received a considerable amount of attention in biosensing. However, most of them are synthesized by immobilizing multiple DNA walking strands on the surface of Au nanoparticles, which is tedious and time-consuming. Simple preparation of multipedal DNA walkers remains a challenge. Herein, we adopted a simple enzyme-free target-triggered catalytic hairpin assembly (CHA) circuit to synthesize a tripedal DNA walker. By walking on a DNA track-functionalized electrode, a sensitive electrochemiluminescence DNA nanomachine biosensor was constructed for sensing miRNA-21. The DNA walker was powered by toehold-mediated strand displacement; the whole process did not need the assistance of enzymes, thus avoiding tedious procedures and enzyme degradation under unfavorable environmental conditions. Specifically, a superior detection limit of 4 aM and a broad linear range of 10 aM to 1 pM were achieved. This CHA−tripedal DNA walker biosensor was then applied for the detection of miRNA-21 in human serum and showed high selectivity and excellent reproducibility, demonstrating its practical application in bioanalysis. In particular, the Y-shaped tripedal DNA walker comes from the DNA circuit, which makes the approach ideally suited for biosensing of small nucleic acid targets.

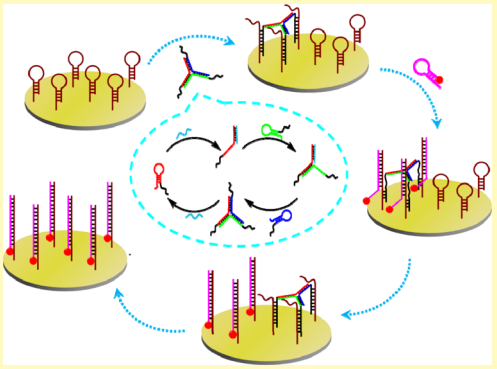

KEYWORDS: *catalytic hairpin assembly, tripedal DNA walker, electrochemiluminescence, miRNA-21, enzyme-free*

MicroRNAs (miRNAs) are a group of endogenous small noncoding RNAs that participate in the regulation of post-transcriptional gene expression in a variety of biological processes. They have been considered as important biomarkers of diseases such as cancers and cardiovascular and autoimmune diseases.[1−4] However, the accurate detection and quantification of miRNAs is a challenge because of the small size, extremely low expression, high homology, and susceptibility to degradation of miRNA.[5,6] Although traditional methods including quantitative reverse transcription polymerase chain reaction, microarray analysis, and northern blotting have been exploited to determine the levels of miRNA expression, their application has been limited by high cost, complicated operation, poor sensitivity, and false-positive results.[7,8] To overcome these shortcomings, several novel techniques, including surface-enhanced Raman spectroscopy,[9] fluorescence,[10] electrochemistry,[11] and electrochemiluminescence (ECL),[12] for the detection of miRNA have been developed. Nevertheless, these techniques alone, without any amplification, are not sensitive enough to detect low-abundance miRNAs. Therefore, utilizing amplification protocols to improve the detection sensitivity of these methods is of particular interest in current research.

Among various amplification techniques, DNA walkers, a type of the autonomous molecular machines, have attracted particular attention owing to the characteristic of the cascade signal enhancement generated by their autonomous movement.[13−20] For a typical DNA walker, the target can trigger a specific DNA walking strand to move continuously and automatically along the predesigned DNA tracks. To date, most DNA walkers have been based on one nanomachine with one walking strand so called the single-leg DNA walkers, which suffer from a limited walking area and slow response kinetics.[14,21] From an analytical point of view, rapid walking kinetics and high processivity facilitate high signal gain in a given period of time.[22] To achieve high processivity and fast response, researchers have developed multipedal DNA walkers by attaching multiple walking strands on the same matrix. In

Received: September 5, 2020
Accepted: October 27, 2020

Scheme 1. Schematic Illustration of ECL miRNA-21 Detection Based on the CHA–Tripedal DNA Walker Strategy; (A) Generation Process of the Tripedal DNA Walker; (B) Walking Process of the Tripedal DNA Walker on the Electrode

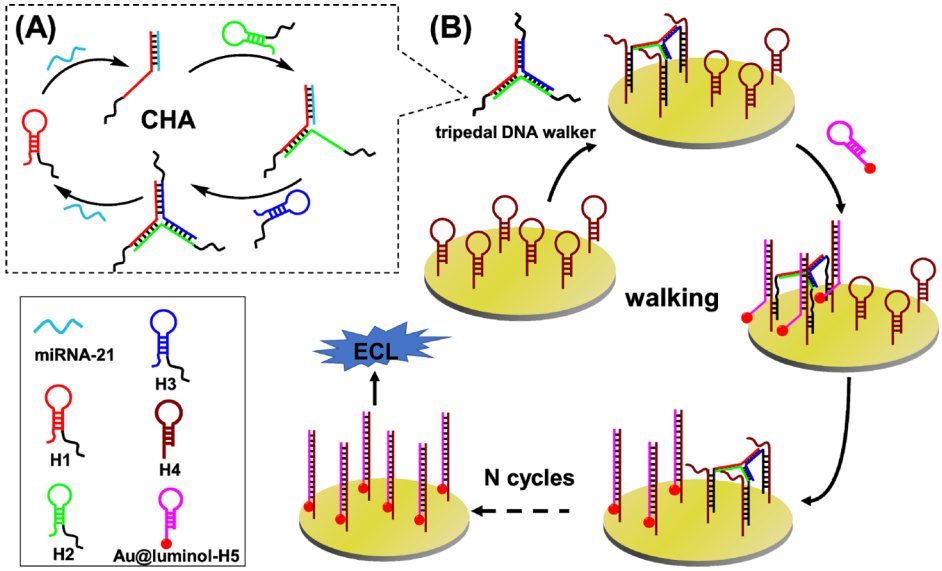

such walkers, the walking rate or distance has been greatly increased with the addition of more "legs". Nevertheless, almost all researched multipedal DNA walkers have been limited to a DNA-functioned gold nanoparticle (AuNP) structure by immobilizing multiple DNA walker strands on AuNPs through Au–S bonds.[21−25] The synthesis procedures for DNA-AuNP composites require several steps of salt aging, centrifugation, and washing, which is cumbersome and time-consuming. Therefore, the facile preparation of multipedal DNA walkers remains a challenge.

Furthermore, the motion of a DNA walker is usually propelled by DNAzyme/endonuclease-mediated hydrolysis and toehold-mediated strand displacement (TMDR).[14,26−29] It is worth noting that the protease/DNAzyme reaction is easily affected by a variety of factors, such as temperature, pH, ion concentration, and so forth, which may affect the walking efficiency and limit its practical application. In contrast, strand displacement is a promising alternative for constructing DNA nanomachines that can achieve reliable motion without being disturbed by environmental factors.[30]

Herein, we introduce an extremely simple yet effective catalytic hairpin assembly (CHA) method to prepare a tripedal walker, which was formed through DNA self-assembly during one incubation, and no conjugation of the DNA walking strand to AuNPs is needed. The CHA-formed tripedal DNA walker is propelled by a toehold exchange reaction to move on a track strand-functionalized electrode and thus to make possible the ECL biosensing of low-abundance miRNA. The whole process does not need the assistance of enzymes, so it can avoid tedious procedures and enzyme degradation under unfavorable environmental conditions. More importantly, the detection sensitivity is much higher than that of most reported DNA walking machine methods owing to the integration of a tripedal DNA walker and CHA circuit cascade signal amplification.

EXPERIMENTAL SECTION

Reagents and Apparatus. The chemical reagents and apparatus are shown in the Supporting Information. Table S1 lists all the DNA and miRNA sequences used in the experiment.

Preparation of Au@luminol. Au@luminol NPs were prepared as previously reported.[31] Briefly, 0.9 mL of luminol (10 mM) was added to 50 mL of boiling $HAuCl_4$ solution (0.01%) under vigorous stirring. The mixture was boiled for 30 min to yield colloidal Au@luminol NPs. After cooling to room temperature, Au@luminol was stored at 4 °C for further use.

Preparation of Au@luminol-HP5. Ten microliters of HP5 solution (100 μM) was mixed with 2 μL of tris(2-carboxyethyl)-phosphine hydrochloride (TCEP) (1 mM) and incubated in the dark for 1 h. Then, 1 mL of Au@luminol solution was added to the above mixture and incubated at 37 °C for 2 h. The synthesized Au@luminol-HP5 was centrifuged, washed with water, and resuspended in 1 mL of phosphate buffer saline (PBS, 0.1 M, pH 7.4) for further use.

Preparation of the Tripedal DNA Walker. For the self-assembly of the tripedal DNA walker, 10 μL of different concentrations of target miRNA-21 and 15 μL of 1 nM hairpin DNAs (5 μL HP1, 5 μL HP2, and 5 μL HP3, respectively) were kept at 37 °C for 4 h to form a stable tripedal DNA walker for further experiments.

Fabrication of the Biosensor. The Au electrode (AuE) was polished with 0.3 and 0.05 μm alumina slurries and then washed ultrasonically in ethanol and ultrapure water. To further clean it, the resulting electrode was scanned from 0 to +1.5 V in 0.5 M H_2SO_4 until a notable voltammetric peak was obtained. Then, in the process of electrode modification, 5 μL of 2 μM DNA track (HP4) pretreated with 10 mM TCEP was modified on the cleaned electrode by the Au–S bond at 4 °C for 12 h. Then, the modified electrode was immersed in a 1 mM MCH solution for 1 h to block the nonspecific sites. When the electrode was completely rinsed with PBS, the obtained biosensor was used to monitor different concentrations of the target miRNA-21 solution.

ECL Measurement Procedure. To measure the ECL response of the proposed biosensor, 5 μL of tripedal DNA walker and 5 μL of 1 μM Au@luminol-HP5 were cast onto the electrode at the same time and incubated for 40 min to walk the tripedal DNA walker. After rinsing, the ECL signal of well-prepared AuE was recorded in PBS (pH 7.4) containing 100 mM H_2O_2.

RESULTS AND DISCUSSION

The characterization of Au@luminol is described in the Supporting Information (Figure S1).

Principle of the CHA–Tripedal DNA Walker ECL Biosensor. The principle of the fabricated ECL biosensor is

https://dx.doi.org/10.1021/acssensors.0c01864
ACS Sens. XXXX, XXX, XXX−XXX

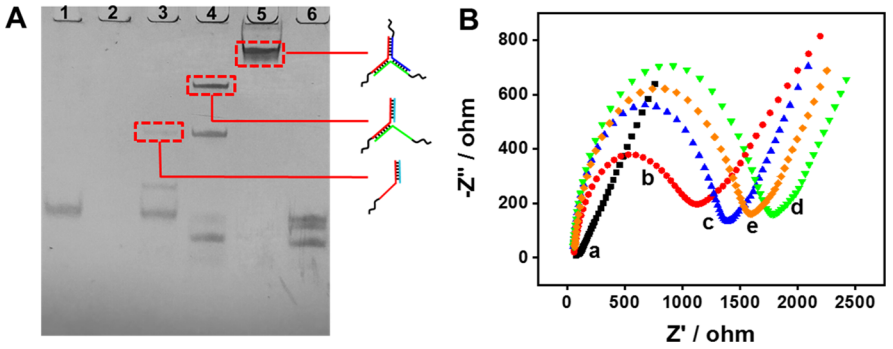

Figure 1. (A) Native PAGE images of different samples. Lane 1: HP1; lane 2: miRNA; lane 3: miRNA + HP1; lane 4: miRNA + HP1 + HP2; lane 5: miRNA + HP1 + HP2 + HP3; lane 6: HP1 + HP2 + HP3. The total volume of all samples was 10 μL, and the concentration of DNA was 2 μM and miRNA-21 was 100 nM. (B) EIS characterization for the stepwise fabrication of the proposed biosensor. (a) Bare AuE; (b) HP4/AuE; (c) MCH/HP4/AuE; (d) tripedal DNA walker/MCH/HP4/AuE; (e) Au@luminol-HP5/tripedal DNA walker/MCH/HP4/AuE.

schematically illustrated in Scheme 1. The whole sensing strategy could be simply divided into two modules: preparation of the tripedal DNA walker and walking machine movement on the surface of the electrode.

As shown in Scheme 1A, the tripedal DNA walker was prepared by target-triggered CHA[32] using target miRNA-21 and three well-designed hairpins, HP1, HP2, and HP3, that have the same ssDNA sequences (black) at their 3′-end. The CHA cycle begins with miRNA-21 binding to HP1, which opens the hairpin structure of HP1 (red) and exposes its initially blocked toehold region. The newly exposed toehold region of HP1 binds HP2 (green) and triggers a second strand-displacement reaction to form the target−HP1−HP2 hybrid and release the toehold region of HP2. HP3 (blue) is opened in the same way, and its toehold section is also exposed. Subsequently, the freed toehold sequence of HP3 hybridizes with HP1 to form Y-shaped DNA (HP1−HP2−HP3) and releases bound miRNA-21 for the next round of reactions. This cyclic process continues autonomously until all HPs are assembled into Y-shaped DNAs. The formed Y-shaped DNA equipped with three ssDNA ends (legs) is called a tripedal DNA walker.

In the walking step (Scheme 1B), the surface of AuE is conjugated with thousands of hairpin DNA strands (HP4) to serve as DNA tracks. The "legs" of the tripedal DNA walker hybridize with HP4 and expose its toehold region. The exposed toehold domain of H4 can interact with Au@luminol-HP5 through a strand displacement reaction, resulting in the formation of a thermodynamically favorable configuration of the HP4/HP5 duplex and the release of "legs" for continued walking. As a result, HP4 is transferred to the HP4/Au@luminol-HP5 duplex, a large amount of Au@luminol is fixed on the electrode surface, and then a significantly amplified ECL signal is obtained.

Viability Analysis. The viability of the proposed strategy was first investigated by native polyacrylamide gel electrophoresis (PAGE) analysis. The CHA self-assembly process of tripedal DNA walker formation is shown in Figure 1A. Lanes 1−5 contain HP1, miRNA-21, miRNA-21 + HP1, miRNA-21 + HP1 + HP2, and miRNA-21 + HP1 + HP2 +HP3, respectively. The band indicated by the red box confirmed the successful progressive hybridization. The migration band is not observed in lane 2 due to the short single-stranded structure of miRNA-21. The final self-assembled tripedal DNA walker exhibited extremely low mobility, while the hairpin probe bands disappeared in lane 5, confirming that the tripedal DNA walker was completely formed by the introduction of miRNA-21. In contrast, in the absence of the target miRNA-21, the hairpin probes HP1, HP2, and HP3 remained stable (lanes 6).

The strand-displacement-driven walking process was also analyzed by PAGE, and the results are shown in Figure S2. Lanes 1−8 contain HP4, HP5, and the mixtures of HP4 + HP5 with other hairpin structures (HP1, HP2, and HP3) or tripedal DNA walkers. From the results, we can see that only the tripedal DNA walker can induce the reaction between HP4 and HP5 by a strand displacement reaction to form the HP4/HP5 duplex, resulting in the disappearance of the HP4 and HP5 bands, thus confirming that the walking process was successful. To further exemplify the walking capability of the tripedal DNA walker, a conventional fluorescent method was employed (Figure S3). For this purpose, FAM-labelled thiolated HP4-modified AuNPs (HP4-AuNPs) were recruited as a well-designed track. In the initiation state, the fluorescence of FAM was quenched by AuNPs owing to a position close to the surface of AuNPs. During the walking process of the tripedal DNA walker on AuNPs, the dissociative HP5 could hybridize with unfolded HP4 and release the "leg" of the tripedal DNA walker, resulting in the production of plentiful HP4−HP5 duplexes. The rigid duplex structure of HP4−HP5 kept FAM away from AuNPs, leading to the recovery fluorescence of FAM. As time extends, the fluorescence signal increased continuously, which could definitively indicate the walking capability of the tripedal DNA walker.

Characterization of the Formation Process of the ECL Biosensor. EIS measurements were employed to embellish the ECL biosensor. Figure 1B indicates the corresponding impedance curve changes with stepwise modification of AuE. An extremely small electron-transfer resistance (R_{et}) was observed from the bare AuE (curve a), which is a result of the fast electron transfer procedure of $[Fe(CN)_6]^{3-/4-}$. When HP4 was immobilized on AuE, an obvious increase in R_{et} was observed, while the negatively charged DNA prevented $[Fe(CN)_6]^{3-/4-}$ from approaching the AuE (curve b). A further enhancement of the value of R_{et} was obtained after treatment with nonconductive MCH (curve c). Sequentially, when the modified AuE was incubated with a mixture containing a tripedal DNA walker, an obvious increase in R_{et} (curve d) could be seen due to the hybridization of the overhanging part of the tripedal DNA walker with HP4. Finally, when Au@luminol-HP5 replaced the tripedal DNA walker on the electrode, a remarkable decrease in R_{et} was observed (curve e), owing to the outstanding electrical

https://dx.doi.org/10.1021/acssensors.0c01864
ACS Sens. XXXX, XXX, XXX−XXX

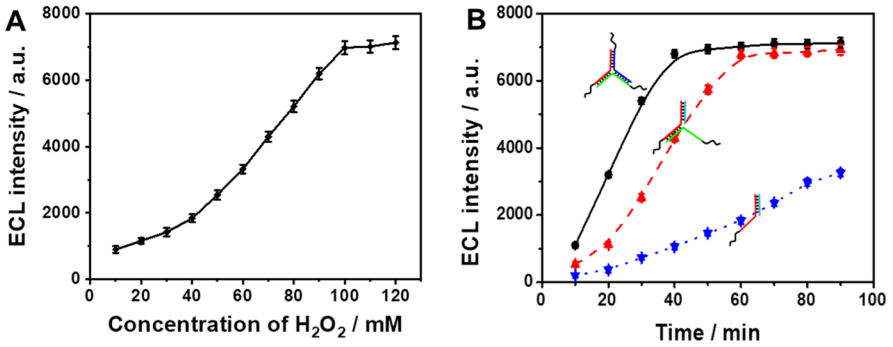

Figure 2. (A) Effect of H_2O_2 concentration on the ECL performance of the tripedal DNA walker biosensor. (B) ECL responses of the tripedal DNA walker, bipedal walker, and unipedal walker. miRNA-21 concentration: 1 pM.

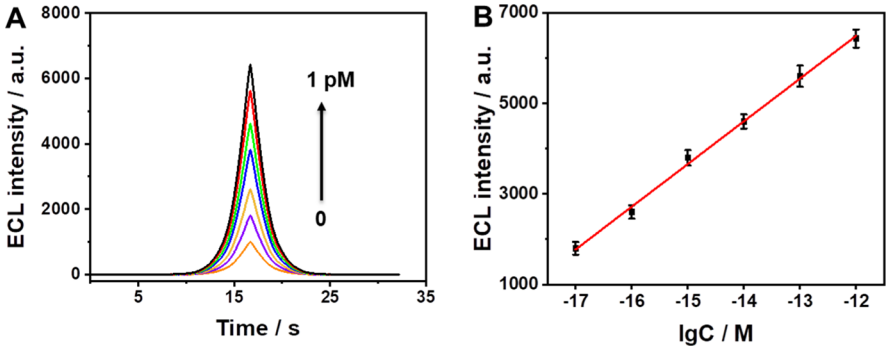

Figure 3. (A) ECL−time curves of different concentrations of miRNA-21 (0, 10^{-17}, 10^{-16}, 10^{-15}, 10^{-14}, 10^{-13} and 10^{-12} M). (B) Calibration plot of the ECL intensity vs lgCmiRNA-21 [(C) 10^{-17}, 10^{-16}, 10^{-15}, 10^{-14}, 10^{-13} and 10^{-12} M].

Table 1. Comparison of Recent DNA Walker-Based Methods for miRNAs Detection

DNA walker type	detection methods	target	detection limit	references
dual-enzyme-driven single-leg walker	fluorescent	miRNA-892b	4.0 pM	13
TMDR-driven single-leg walker	fluorescent	miRNA-21	4.0 pM	14
enzyme-driven single-leg walker	photoelectrochemical	miRNA-141	0.6 fM	15
enzyme-driven single-leg walker	fluorescent	miRNA-21	1.67 fM	16
DNAzyme-driven single-leg walker	fluorescent	miRNA-21	34.0 pM	17
enzyme-driven walker	electrochemical	miRNA-155/miRNA-21	42.7/51.1 aM	18
DNAzyme-driven bipedal walker	ECL	miRNA-155	12.2 aM	19
TMDR-driven bipedal walker	ECL	miRNA-21	0.24 pM	20
TMDR-driven unipedal walker	ECL	miRNA-21	1.6 pM	this work
TMDR-driven bipedal walker	ECL	miRNA-21	10.0 fM	this work
TMDR-driven tripedal walker	ECL	miRNA-21	4.0 aM	this work

conductivity of AuNPs. In summary, the EIS results can definitively indicate the successful fabrication of the proposed biosensor.

Optimization of the Experimental Conditions. To realize the best performance of the sensor for miRNA-21 detection, the effects of HP4 and Au@luminol-HP5 concentration on the performance of Au@luminol ECL were first studied. As shown in Figure S4A, the ECL intensity increased with increasing HP4 concentration and reached a plateau at 2.0 μM. Thus, the concentration of 2.0 μM was chosen as the optimum condition of HP4. Similarly, the optimum concentration of Au@luminol-HP5 was 1.0 μM, as shown in Figure S4B. Some other conditions including a concentration of 1 nM hairpin DNAs (HP1, HP2, and HP3) and an assembly time of 4 h to generate the tripedal DNA walker were also optimized as shown in Figure S4C,D.

The coreactant (H_2O_2) concentration and the walking time of the tripedal DNA walker were other vital factors affecting the performance of the sensors. As shown in Figure 2A, the ECL intensity of Au@luminol gradually increased with increasing concentration of the coreactant H_2O_2 from 10 to 100 mM and nearly stabilized at 100 mM and above. Thus, 100 mM H_2O_2 was chosen in this work. As displayed in Figure 2B, the ECL signal increased rapidly when the walking time increased from 10 to 40 min and subsequently maintained a relatively stable value. Therefore, the walking time of the tripedal DNA walker on the electrode surface was set at 40 min for the subsequent study. Compared with bipedal and unipedal walkers, the tripedal DNA walker shows the highest walking speed since more "legs" on a DNA walker allow higher rates.[24] The comparison results are shown in Figure 2B. The tripedal DNA walker exhibited the fastest signal variation rate and reached a plateau in 40 min. The bipedal DNA walker reached equilibrium in 60 min, but the single-leg DNA walker was still working after 60 min.

https://dx.doi.org/10.1021/acssensors.0c01864
ACS Sens. XXXX, XXX, XXX−XXX

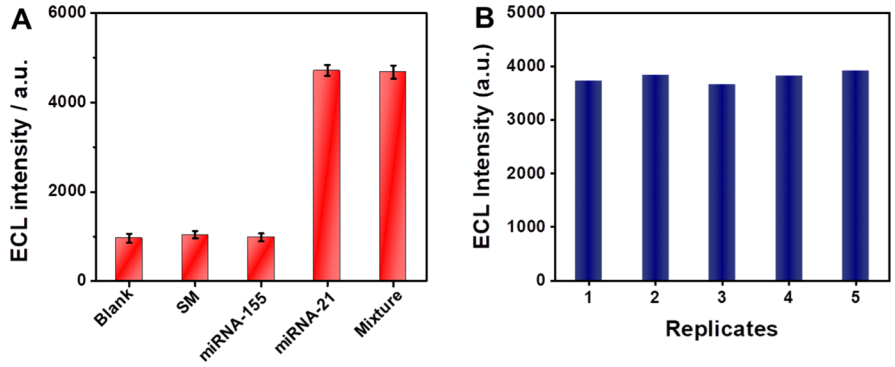

Figure 4. (A) Selectivity evaluation for the proposed biosensor. SM: single-base-mismatched miRNA-21. (B) Reproducibility of the proposed biosensor with five electrodes (1 fM miRNA-21).

Detection of miRNA-21. The biosensor was used to quantitatively determine the concentration of miRNA-21 under the optimal conditions. As shown in Figure 3A, the ECL intensity gradually increased with increasing miRNA-21 concentration from 0 to 1 pM. A linear relationship of the ECL intensity was observed and was dependent on the logarithmic value of miRNA-21 concentration ranging from 10 aM to 1 pM with a correlation coefficient of 0.9977 (Figure 3B). The detection limit (LOD) was estimated to be 4 aM (S/N = 3). Compared with some DNA walker methods for miRNA detection in previous reports (Table 1), the unipedal walker and bipedal walker used in this work and the proposed CHA−tripedal DNA walker ECL biosensor exhibited a lower detection limit, making it more promising for application in early diagnosis.

Selectivity, Reproducibility, and Storage Stability of the Proposed ECL Biosensor. To evaluate the selectivity of the developed biosensor, single-base-mismatched miRNA-21 and miRNA-155 were chosen as interfering agents. As shown in Figure 4A, significant ECL signals were observed only in the presence of miRNA-21 (1 fM), either with miRNA-21 alone or in a mixture containing miRNA-21 samples. The incubation of the biosensor with interference substances (1 nM) gave a negligible signal. The results above indicated that only completely complementary miRNA-21 could trigger CHA to form a tripedal DNA walker efficiently and lead to an increase in ECL intensity, which demonstrates the desirable differentiation capability toward target miRNA-21.

To investigate the reproducibility of the ECL biosensor, five proposed biosensor electrodes from the same batches were analyzed by repeated detection of 1 fM target miRNA-21 under the same experimental conditions. The relative standard deviation (RSD) was 2.4% (Figure 4B), indicating that the proposed biosensor had satisfactory reproducibility. The storage stability of the proposed biosensor after two weeks of storage (at 4 °C) was investigated. No significant change in ECL intensity was observed, which suggested that the biosensor was reliable and stable.

Detection of miRNA-21 in Serum Samples. To test the practical applicability, different concentrations of miRNA-21 were added to the diluted human serum (10 times with PBS), and the analysis results are shown in Table 2. The recoveries were between 95.0 and 102.4%, while RSD ranged from 2.9 to 5.3%, demonstrating the favorable practicality in complex real samples.

Table 2. Serum Sample Analysis for the Proposed Biosensor

sample	added	detected	recovery (%)	RSD (%)
1	100.0 aM	98.3 aM	98.3	4.2
2	500.0 aM	475.0 aM	95.0	2.9
3	10.0 fM	9.6 fM	96.0	4.8
4	50.0 fM	51.2 fM	102.4	5.3
5	100.0 fM	98.9 fM	98.9	3.2

CONCLUSIONS

In summary, a simple tripedal DNA walker was designed and applied for an ECL biosensor to selectively and sensitively detect miRNA-21. The tripedal DNA walker was activated by the CHA assembly, forming a Y-shaped structure with three "legs" in the presence of miRNA-21, and walked on a DNA track-functionalized electrode, producing a significant ECL. Unlike the previously studied multipedal DNA walker, our tripedal DNA walker does not require complex process of immobilization of walker DNA on the NPs. Taking advantage of CHA and tripedal DNA walker dual signal amplification, high sensitivity for miRNA-21 detection was achieved. This biosensor exhibited excellent selectivity and was successfully applied to detect miRNA-21 in human serum samples. In addition, this strategy possesses very good extensibility by using corresponding DNA hairpins to hybridize with the targets for the formation of a tripedal DNA walker, indicating its promising application for detecting various nucleic acids (RNA and DNA).

ASSOCIATED CONTENT

Supporting Information

The Supporting Information is available free of charge at https://pubs.acs.org/doi/10.1021/acssensors.0c01864.

Materials and reagents; apparatus and measurements; sequences of the oligonucleotides used in the experiment; synthesis of AuNPs; preparation of FAM-HP4-modified AuNPs; fluorescent analysis of the walking process of tripedal DNA walker; characterization of Au@luminol; PAGE analysis of strand-displacement-driven TDW walking process; and optimization of detection conditions (PDF)

AUTHOR INFORMATION

Corresponding Authors

Li Wang − *State Key Laboratory of Analytical Chemistry for Life Science, School of Chemistry and Chemical Engineering,*

https://dx.doi.org/10.1021/acssensors.0c01864
ACS Sens. XXXX, XXX, XXX−XXX

Nanjing University, Nanjing 210023, China; School of Pharmacy, Jiangsu University, Zhenjiang 212013, Jiangsu, China; orcid.org/0000-0001-6650-8323; Email: wangjill@126.com

Jun-Jie Zhu − *State Key Laboratory of Analytical Chemistry for Life Science, School of Chemistry and Chemical Engineering, Nanjing University, Nanjing 210023, China;* orcid.org/0000-0002-8201-1285; Email: jjzhu@nju.edu.cn

Authors

Pengfei Liu − *School of Pharmacy, Jiangsu University, Zhenjiang 212013, Jiangsu, China*

Zhijun Liu − *School of Pharmacy, Jiangsu University, Zhenjiang 212013, Jiangsu, China*

Kairen Zhao − *School of Pharmacy, Jiangsu University, Zhenjiang 212013, Jiangsu, China*

Shuying Ye − *School of Environment & Safety Engineering, Jiangsu University, Zhenjiang 212013, Jiangsu, China*

Guoxi Liang − *School of Environment & Safety Engineering, Jiangsu University, Zhenjiang 212013, Jiangsu, China*

Complete contact information is available at: https://pubs.acs.org/10.1021/acssensors.0c01864

Author Contributions

L.W. conceived the experiments, supervised the manuscript, and acquired the funding. P.L. conceived and administrated the experiments, wrote the manuscript, and interpreted the data. Z.L. analyzed the data. K.Z. validated the data. S.Y. implemented the figures. G.L. supervised the manuscript. J.-J.Z. supervised the manuscript.

Notes

The authors declare no competing financial interest.

■ ACKNOWLEDGMENTS

This work was financially supported by the National Natural Science Foundation of China (no. 21707053).

■ REFERENCES

(1) Jeffrey, S. S. Cancer biomarker profiling with microRNAs. *Nat. Biotechnol.* **2008**, *26*, 400−401.

(2) Mitchell, P. S.; Parkin, R. K.; Kroh, E. M.; Fritz, B. R.; Wyman, S. K.; Pogosova-Agadjanyan, E. L.; Peterson, A.; Noteboom, J.; O'Briant, K. C.; Allen, A.; Lin, D. W.; Urban, N.; Drescher, C. W.; Knudsen, B. S.; Stirewalt, D. L.; Gentleman, R.; Vessella, R. L.; Nelson, P. S.; Martin, D. B.; Tewari, M. Circulating microRNAs as stable blood-based markers for cancer detection. *Proc. Natl. Acad. Sci. U.S.A.* **2008**, *105*, 10513−10518.

(3) Tijsen, A. J.; Pinto, Y. M.; Creemers, E. E. Circulating microRNAs as diagnostic biomarkers for cardiovascular diseases. *Am. J. Physiol. Heart Circ. Physiol.* **2012**, *303*, H1085−H1095.

(4) Kosaka, N.; Iguchi, H.; Ochiya, T. Circulating microRNA in body fluid: a new potential biomarker for cancer diagnosis and prognosis. *Cancer Sci.* **2010**, *101*, 2087−2092.

(5) Wark, A. W.; Lee, H. J.; Corn, R. M. Multiplexed detection methods for profiling microRNA expression in biological samples. *Angew. Chem., Int. Ed.* **2008**, *47*, 644−652.

(6) Yu, Y.; Chen, Z.; Shi, L.; Yang, F.; Pan, J.; Zhang, B.; Sun, D. Ultrasensitive electrochemical detection of microRNA based on an arched probe mediated isothermal exponential amplification. *Anal. Chem.* **2014**, *86*, 8200−8205.

(7) Dong, H.; Lei, J.; Ding, L.; Wen, Y.; Ju, H.; Zhang, X. MicroRNA: function, detection, and bioanalysis. *Chem. Rev.* **2013**, *113*, 6207−6233.

(8) Wei, T.; Du, D.; Wang, Z.; Zhang, W.; Lin, Y.; Dai, Z. Rapid and sensitive detection of microRNA via the capture of fluorescent dyes-loaded albumin nanoparticles around functionalized magnetic beads. *Biosens. Bioelectron.* **2017**, *94*, 56−62.

(9) Zhou, W.; Tian, Y.-F.; Yin, B.-C.; Ye, B.-C. Simultaneous surface-enhanced Raman spectroscopy detection of multiplexed microRNA biomarkers. *Anal. Chem.* **2017**, *89*, 6120−6128.

(10) Wang, H.; Wang, H.; Wu, Q.; Liang, M.; Liu, X.; Wang, F. A DNAzyme-amplified DNA circuit for highly accurate microRNA detection and intracellular imaging. *Chem. Sci.* **2019**, *10*, 9597−9604.

(11) Xu, S.; Chang, Y.; Wu, Z.; Li, Y.; Yuan, R.; Chai, Y. One DNA circle capture probe with multiple target recognition domains for simultaneous electrochemical detection of miRNA-21 and miRNA-155. *Biosens. Bioelectron.* **2020**, *149*, 111848.

(12) Zhang, Y.; Xu, G.; Lian, G.; Luo, F.; Xie, Q.; Lin, Z.; Chen, G. Electrochemiluminescence biosensor for miRNA-21 based on toehold-mediated strand displacement amplification with Ru-$(phen)_3^{2+}$ loaded DNA nanoclews as signal tags. *Biosens. Bioelectron.* **2020**, *147*, 111789.

(13) Chen, T.; Chen, Y.; Chen, H.; Zhang, F.; Zhang, Q.; Chen, G.; Zhu, X. Dual-enzyme-propelled unbounded DNA walking nanomachine for intracellular imaging of lowly expressed microRNA. *Nano Res.* **2019**, *12*, 1055−1060.

(14) Oishi, M.; Saito, K. Simple single-legged DNA walkers at diffusion-limited nanointerfaces of gold nanoparticles driven by a DNA circuit mechanism. *ACS Nano* **2020**, *14*, 3477−3489.

(15) Li, L.; Zhang, Y.; Yan, Z.; Chen, M.; Zhang, L.; Zhao, P.; Yu, J. Ultrasensitive photoelectrochemical detection of microRNA on paper by combining a cascade nanozyme-engineered biocatalytic precipitation reaction and target-triggerable DNA motor. *ACS Sens.* **2020**, *5*, 1482−1490.

(16) Xiao, M.; Wang, X.; Li, L.; Pei, H. Stochastic RNA walkers for intracellular microRNA imaging. *Anal. Chem.* **2019**, *91*, 11253−11258.

(17) Liu, C.; Hu, Y.; Pan, Q.; Yi, J.; Zhang, J.; He, M.; He, M.; Chen, T.; Chu, X. A microRNA-triggered self-powered DNAzyme walker operating in living cells. *Biosens. Bioelectron.* **2019**, *136*, 31−37.

(18) Chang, Y.; Wu, Z.; Sun, Q.; Zhuo, Y.; Chai, Y.; Yuan, R. Simply constructed and highly efficient classified cargo-discharge DNA robot: a DNA walking nanomachine platform for ultrasensitive multiplexed sensing. *Anal. Chem.* **2019**, *91*, 8123−8128.

(19) Liu, D.; Zhang, X.; Zhao, J.; Chen, S.; Yuan, R. An ultrasensitive sensing platform for microRNA-155 based on H2O2 quenched hydroxide-dependent ECL emission of PFO Pdots. *Biosens. Bioelectron.* **2020**, *150*, 111872.

(20) Chen, A.; Zhuo, Y.; Chai, Y.; Yuan, R. Bipedal DNA walker mediated enzyme-free exponential isothermal signal amplification for rapid detection of microRNA. *Chem. Commun.* **2019**, *55*, 13932−13935.

(21) Zhang, H.; Xu, X.; Jiang, W. An interparticle relatively motional DNA walker and its sensing application. *Chem. Sci.* **2020**, *11*, 7415−7423.

(22) Zhou, R.; Hu, C.; Jin, Y.; Zhang, J.; Du, H.; Yang, P.; Chen, J.; Hou, X.; Cheng, N. Spatially constrained DNA nanomachines to accelerate kinetics in response to external input: design and bioanalysis. *Anal. Chem.* **2020**, *92*, 8909−8916.

(23) Miao, P.; Tang, Y. Gold nanoparticles-based multipedal DNA walker for ratiometric detection of circulating tumor cell. *Anal. Chem.* **2019**, *91*, 15187−15192.

(24) Xu, Z.; Chang, Y.; Chai, Y.; Wang, H.; Yuan, R. Ultrasensitive electrochemiluminescence biosensor for speedy detection of microRNA based on a DNA rolling machine and target recycling. *Anal. Chem.* **2019**, *91*, 4883−4888.

(25) Li, D.; Xu, Y.; Fan, L.; Shen, B.; Ding, X.; Yuan, R.; Li, X.; Chen, W. Target-driven rolling walker based electrochemical biosensor for ultrasensitive detection of circulating tumor DNA using doxorubicin@tetrahedron-Au tags. *Biosens. Bioelectron.* **2020**, *148*, 111826.

(26) Jung, C.; Allen, P. B.; Ellington, A. D. A stochastic DNA walker that traverses a microparticle surface. *Nat. Nanotechnol.* **2016**, *11*, 157−163.
(27) Peng, H.; Li, X. F.; Zhang, H.; Chris Le, X. A microRNA-initiated DNAzyme motor operating in living cells. *Nat. Commun.* **2017**, *8*, 14378.
(28) Li, Y.; Wang, G. A.; Mason, S. D.; Yang, X.; Yu, Z.; Tang, Y.; Li, F. Simulation-guided engineering of an enzyme-powered three dimensional DNA nanomachine for discriminating single nucleotide variants. *Chem. Sci.* **2018**, *9*, 6434−6439.
(29) Zhang, H.; Lai, M.; Zuehlke, A.; Peng, H.; Li, X.-F.; Le, X. C. Binding-induced DNA nanomachines triggered by proteins and nucleic acids. *Angew. Chem., Int. Ed.* **2015**, *54*, 14326−14330.
(30) Chen, J.; Luo, Z.; Sun, C.; Huang, Z.; Zhou, C.; Yin, S.; Duan, Y.; Li, Y. Research progress of DNA walker and its recent applications in biosensor. *TrAC, Trends Anal. Chem.* **2019**, *120*, 115626.
(31) Cheng, Y.; Huang, Y.; Lei, J.; Zhang, L.; Ju, H. Design and biosensing of Mg^{2+}-dependent DNAzyme-triggered ratiometric electrochemiluminescence. *Anal. Chem.* **2014**, *86*, 5158−5163.
(32) Zhu, D.; Huang, J.; Lu, B.; Zhu, Y.; Wei, Y.; Zhang, Q.; Guo, X.; Yuwen, L.; Su, S.; Chao, J.; Wang, L. Intracellular microRNA imaging with MoS_2-supported nonenzymatic catassembly of DNA hairpins. *ACS Appl. Mater. Interfaces* **2019**, *11*, 20725−20733.

https://dx.doi.org/10.1021/acssensors.0c01864
ACS Sens. XXXX, XXX, XXX−XXX